Electronic Supplementary Material (ESI) for Nanoscale.

Supplementary information

Effective-concentration-ratio driven phase engineering of MBE-grown few-layer $MoTe_2$

Kamlesh Bhatt,[a] Santanu Kandar,[a] Nand Kumar,[b] Ashok Kapoor,[a] and Rajendra Singh[* a,b,c]

[a]*Department of Physics, Indian Institute of Technology Delhi, Hauz Khas, New Delhi 110016, India.*

[b]*School of Interdisciplinary Research (SIRe), Indian Institute of Technology Delhi, Hauz Khas, New Delhi 110016, India.*

[c]*Department of Electrical Engineering, Indian Institute of Technology Delhi, Hauz Khas, New Delhi 110016, India.*

[*]*E-mail: rsingh@physics.iitd.ac.in*

S1

The growth was monitored in-situ using RHEED. Initially, sharp RHEED streaks corresponding to the single-crystalline sapphire substrate were obtained. As growth progressed, these streaks faded and a new set of streaks started to evolve, corresponding to 2H-$MoTe_2$.

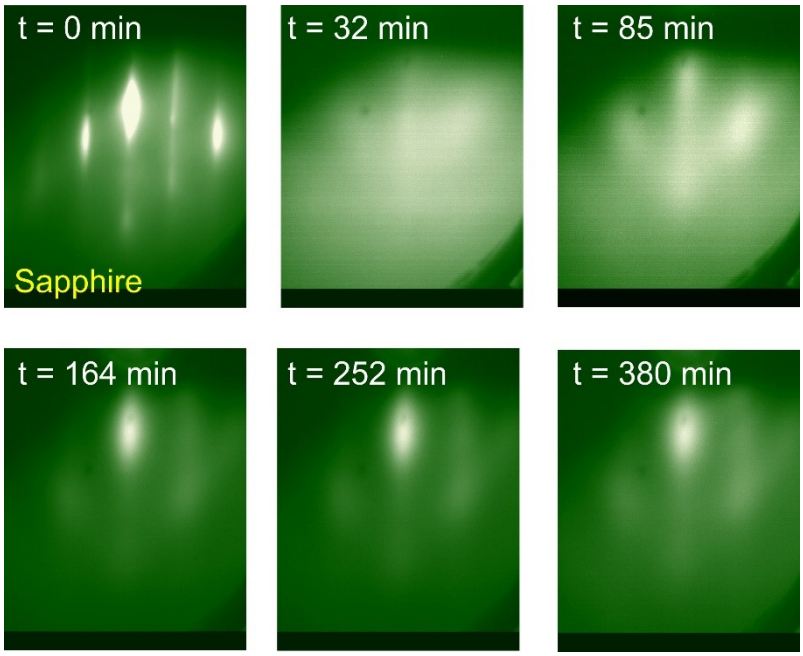

Fig. 1. RHEED evolution showing the emergence of streaky RHEED pattern during the growth

S2

Observation of RHEED intensity oscillations is one of the best ways to estimate layer formation time and layer numbers [1,2]. The layer numbers in a growing film are estimated by observing the change in the intensity of the specular diffraction spot with time over the growth period. The film thickness can be precisely monitored using this intensity profile plot with time, where a maxima corresponds to the completion of the layer. The only requirement for this method is that the growth should take place in layer-by-layer mode,

not in the island mode. Hence, the occurrence of RHEED oscillations also confirms the layer-by-layer growth mode.

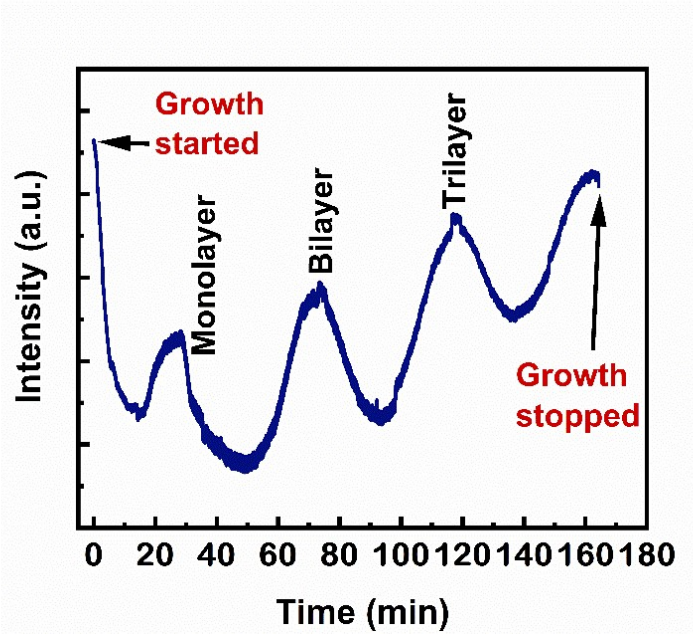

Fig. 2. Observation of RHEED intensity oscillations for estimating layer numbers

S3

We performed the UV-Vis-NIR absorbance spectroscopy for both 2H and 1T' $MoTe_2$ films (Fig. 3). The overall absorbance is very small due to the ultra-thin nature of the grown films, so we did not get any large variation in the absorption data, following nearly similar trend for both. However, slightly distinct features are evident for the two phases. For the 1T' phase, the absorbance increases monotonically with energy without the appearance of any significant feature due to its semimetallic nature. However, for the 2H phase, a prominent increase in the absorbance is observed around its bandgap energy value of ~ 0.8 eV (as indicated by the black arrow). Also, small humps are observed at further higher

energy values (as indicated by red arrows) which correspond to higher energy excitons for the semiconducting phase of $MoTe_2$ [3].

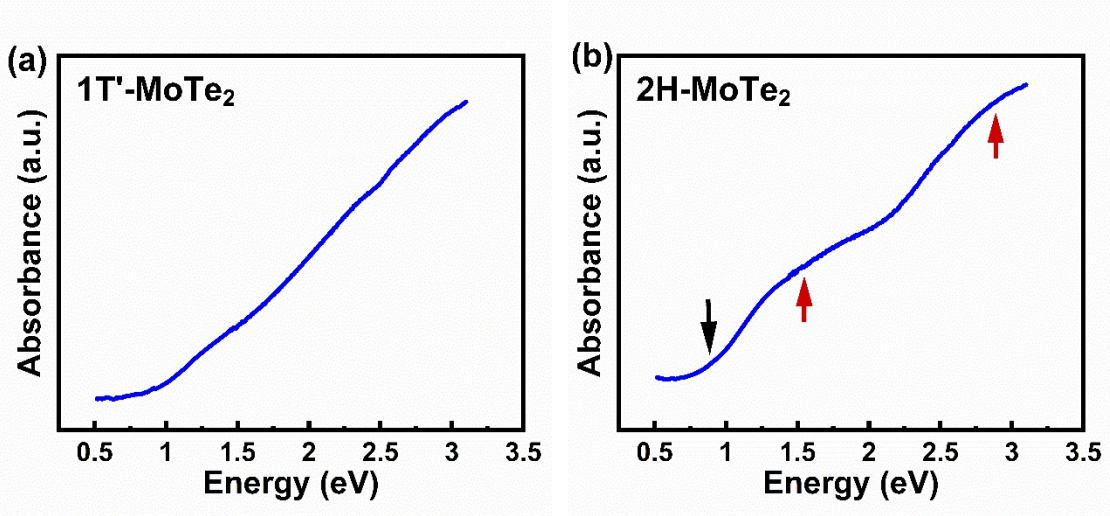

Fig. 3. Vis-NIR absorption spectra of (a) 1T' and (b) 2H $MoTe_2$ grown on a sapphire substrate. The small optical features in the 2H phase are indicated by the arrows.

S4

Glancing incidence (GI) XRD is the preferred mode for ultrathin films because only a limited number of crystalline planes are available for diffraction if normal gonio-XRD is used. However, this mode is limited by the crystallinity of the film, and diffraction can occur only if there is significant polycrystallinity and mosaicity in the film. This is because of the GIXRD configuration where the scattering vector does not remain parallel to the surface normal during the different 2θ values. Hence, a set of planes perfectly parallel to

the surface will not diffract in GIXRD. However, if there is a significant polycrystallinity in the out-of-plane direction, then the reciprocal vector corresponding to these planes will be oriented in all directions and will match with the scattering vector direction.

This is evident in Fig. 4, where no diffraction peak is obtained for 400 °C grown film, while it appears for 450 °C grown film. This indicates that the former has better crystallinity than the latter, which can be further confirmed by the corresponding RHEED pattern, in which comparatively sharper and more resolved diffraction streaks are obtained for a 400 °C grown film.

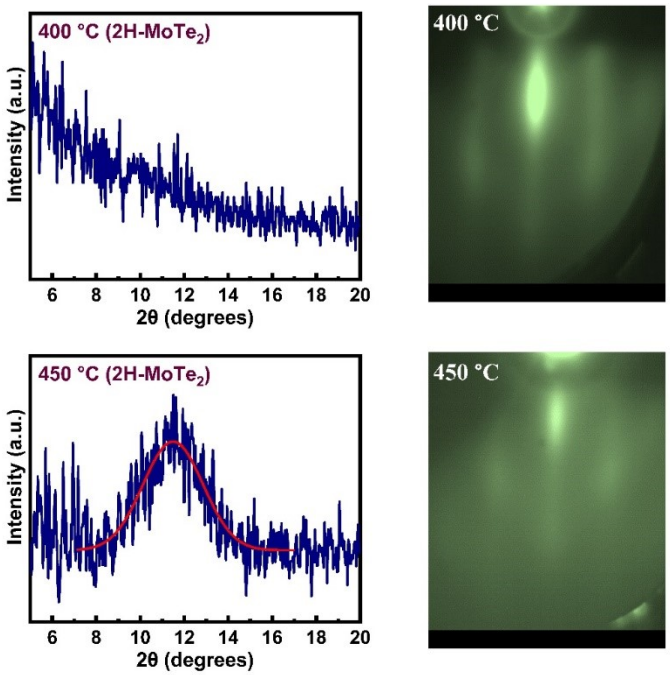

Fig. 4. GI-XRD and corresponding RHEED pattern for the film grown at 400 °C and 450 °C.

S5

To investigate the in-plane lattice parameters, we performed RHEED analysis to calculate in-plane lattice parameters based on the spacing between any one set of RHEED streaks

(Fig. 5). The obtained RHEED pattern shows well-resolved streaks for the 2H phase, while those are slightly diffused for the 1T' phase (the asymmetric intensity is due to the partially coated RHEED screen). It follows AFM results, which show a flat surface for the 2H phase while dense grain boundary defects for the 1T' phase.

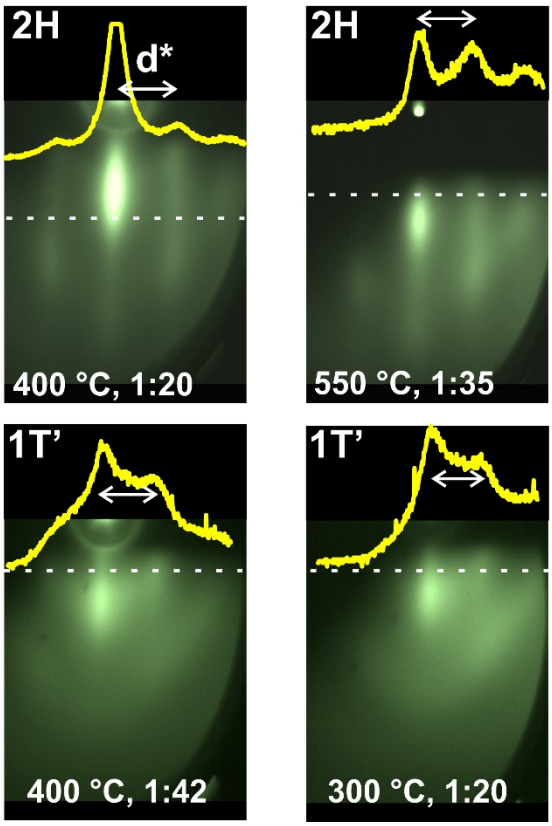

Fig. 5. RHEED images and corresponding intensity profiles for the two phases of $MoTe_2$, which are used to calculate in-plane lattice parameters as shown in supplementary Table 1.

Calculation of in-plane lattice parameters:

Since the interplanar distance is reciprocal to the RHEED spacing ($d \propto 1 / d^*$),

$d(MoTe_2) \times d^*(MoTe_2) = d\,(Sapphire) \times d^*\,(Sapphire)$,

$d(MoTe_2) = d\,(Sapphire) \times d^*\,(Sapphire) / d^*\,(MoTe_2)$,

For sapphire, d (Sapphire) = $\sqrt{3}/2$ a = 4.12 Å and d* (Sapphire) = 88 (length^{-1}),

d($MoTe_2$) = 4.12 (Å) × 88 (length^{-1}) / d* ($MoTe_2$).

Table 1. In-plane lattice parameters calculated from the XRD spectra for different thicknesses

Grown phase (T_G, Mo:Te)	**RHEED spacing for grown films (d*)**	**Calculated value of Lattice spacing (d)**	**In-plane lattice parameter for**	
			2H-$MoTe_2$ ($2/\sqrt{3})d$	**1T'-$MoTe_2$ ($2d$)**
2H (400 °C, 1:20)	118 (length^{-1})	3.07 Å	3.55 Å	-
2H (550 °C, 1:35)	113 (length^{-1})	3.21 Å	3.70 Å	-
1T' (400 °C, 1:42)	105 (length^{-1})	3.45 Å	-	6.90 Å
1T' (300 °C, 1:20)	100 (length^{-1})	3.62 Å	-	7.25 Å

and the two phases of $MoTe_2$ films.

S6

We have achieved a 1T' phase dominant film for a Te-deficient regime of growth parameters. Based on XRD diffraction, a similar substrate effect is evident where the out-of-plane lattice parameter for Te-deficient film is also higher than the bulk value (Fig. 6a). So, this change in the lattice parameter can be assigned to substrate-induced effect, as described previously. However, RHEED analysis shows that the in-plane lattice parameter for Te-deficient films (a = 6.50-6.75 Å) is closer to the bulk values (a = 6.33 Å) than it was for Te-rich films (a = 6.90-7.25 Å) and the film is more relaxed (Fig. 6b). This means that the excess of charge carriers in the case of Te-

deficient films does not affect the lattice parameters of the grown film as much as extra tellurium in the lattice does.

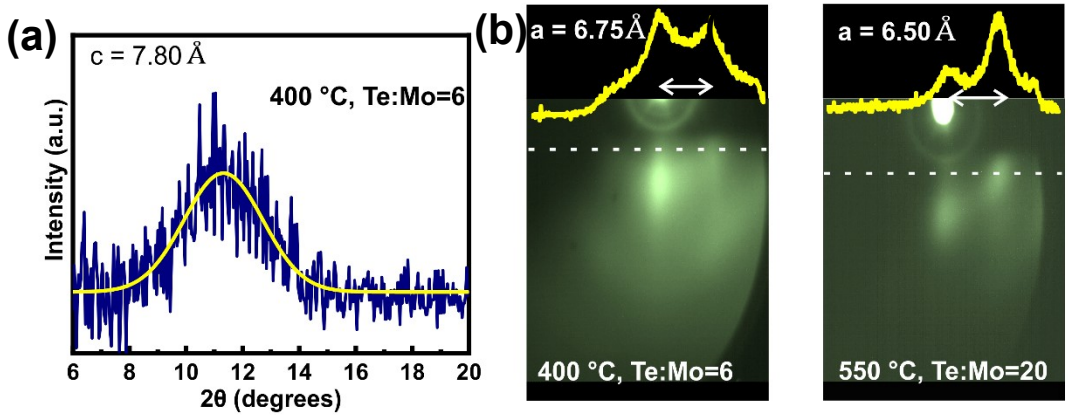

Fig. 6. (a) XRD pattern and (b), (c) RHEED images with intensity profiles for Te deficient films achieved for different growth parameters

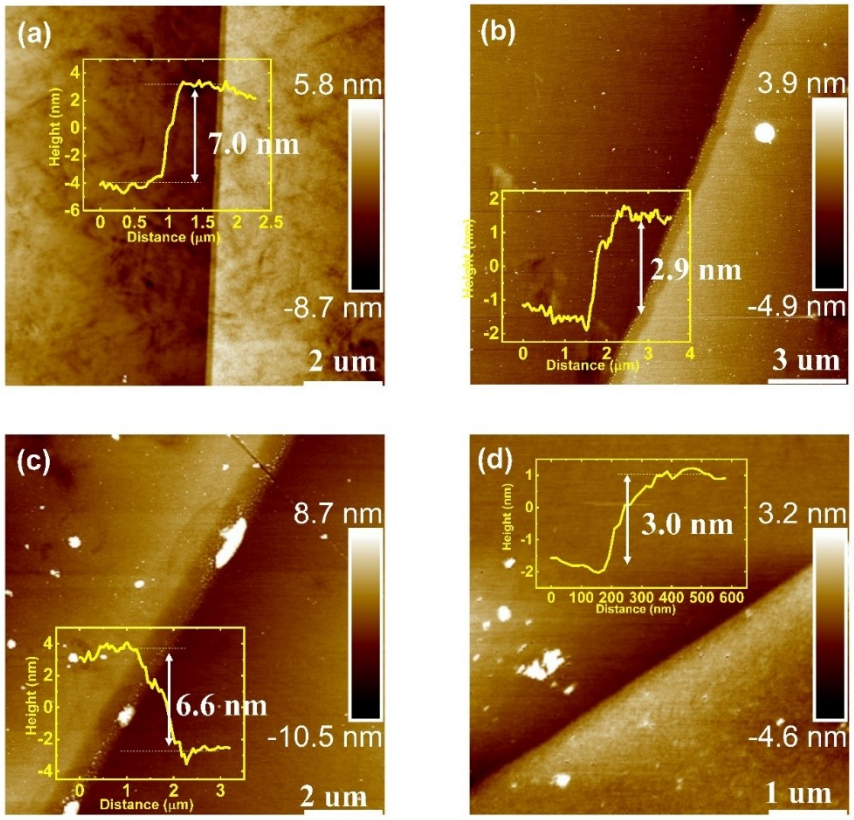

Fig. 7. AFM images and height profiles across the film-substrate step edge confirm the thicknesses of the grown film. Fig. (a) and (c) show a 9-10 layers thick film while (b) and (d) show a 4 layers thick film.

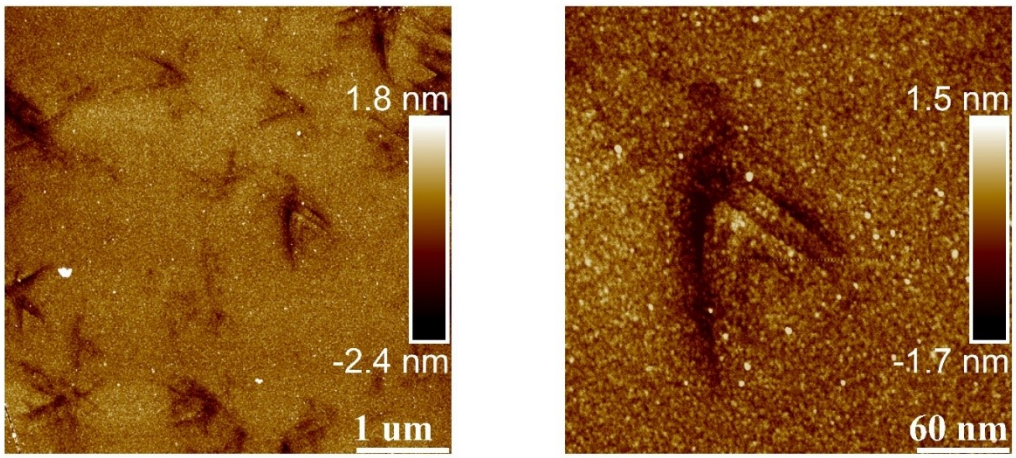

Diffraction plane	Peak position, 2θ (degrees)	
	2H-$MoTe_2$	**1T'-$MoTe_2$**
002	12.18	12.08
004	24.64	24.64
006	37.62	-
008	50.76	-

Fig. 8. Some other than antiparallel triangular features are also observed in 1T'- $MoTe_2$ film, which might have originated from different types of defects such as dislocations.

S9

Table 2. The 2θ peak positions of X-ray diffraction peaks for relatively thicker 2H and 1T' $MoTe_2$ films

S10

Calculation S10. Calculation of work functions for the grown $MoTe_2$ films with different stoichiometry.

KPFM is used to measure the surface potential of the film in terms of contact potential difference (V_{CPD}) between the AFM tip and the sample, which depends on their work functions as follows,

V_{CPD} = WF(tip) – WF(sample) (under sample biased condition)

A freshly exfoliated HOPG, with its standard work function of ~ 4.70 eV, was used to calculate the work function of the tip and the other films. The measured V_{CPD} value for HOPG is 240 mV.

V_{CPD} (HOPG) – V_{CPD} ($MoTe_2$) = WF($MoTe_2$) - WF(HOPG)

WF($MoTe_2$) = V_{CPD} (HOPG) – V_{CPD} ($MoTe_2$) + WF(HOPG)

From Fig. 7,

For Mo:Te = 1:2.0, V_{CPD} ($MoTe_2$) = 240; WF($MoTe_2$) = 4.70 eV

For Mo:Te = 1:1.9, V_{CPD} ($MoTe_2$) = 280; WF($MoTe_2$) = 4.66 eV

For Mo:Te = 1:1.8, V_{CPD} ($MoTe_2$) = 290; WF($MoTe_2$) = 4.65 eV

References:

1 H. Y. Sun, Z. W. Mao, T. W. Zhang, L. Han, T. T. Zhang, X. B. Cai, X. Guo, Y. F. Li, Y. P. Zang, W. Guo, J. H. Song, D. X. Ji, C. Y. Gu, C. Tang, Z. B. Gu, N. Wang, Y. Zhu, D. G. Schlom, Y. F. Nie and X. Q. Pan, *Nat Commun*, 2018, **9**, 2965.

2 I. Leermakers, K. Rubi, M. Yang, B. Kerdi, M. Goiran, W. Escoffier, A. S. Rana, A. E. M. Smink, A. Brinkman, H. Hilgenkamp, J. C. Maan and U. Zeitler, *Journal of Physics: Condensed Matter*, 2021, **33**, 465002.

3 D. P. Gulo, N. T. Hung, R. Sankar, R. Saito and H.-L. Liu, *Phys Rev Mater*, 2023, **7**, 044001.